

WEIGHTED-AVERAGE ALTERNATING MINIMIZATION METHOD FOR MAGNETIC RESONANCE IMAGE RECONSTRUCTION BASED ON COMPRESSIVE SENSING

YONGGUI ZHU

School of Science, Communication University of China
Beijing, 100024, China

YUYING SHI

Department of Mathematics and Physics, North China Electric Power University
Beijing, 102206, China

BIN ZHANG AND XINYAN YU

School of Science, Communication University of China
Beijing, 100024, China

(Communicated by Xuecheng Tai)

ABSTRACT. The problem of compressive-sensing (CS) L2-L1-TV reconstruction of magnetic resonance (MR) scans from undersampled k -space data has been addressed in numerous studies. However, the regularization parameters in models of CS L2-L1-TV reconstruction are rarely studied. Once the regularization parameters are given, the solution for an MR reconstruction model is fixed and is less effective in the case of strong noise. To overcome this shortcoming, we present a new alternating formulation to replace the standard L2-L1-TV reconstruction model. A weighted-average alternating minimization method is proposed based on this new formulation and a convergence analysis of the method is carried out. The advantages of and the motivation for the proposed alternating formulation are explained. Experimental results demonstrate that the proposed formulation yields better reconstruction results in the case of strong noise and can improve image reconstruction via flexible parameter selection.

1. Introduction. Compressive sensing (CS) has enormous potential for reducing the scan time in magnetic resonance image (MRI) research [3, 9]. Sparse signals can be recovered from a very limited number of samples if the measurements satisfy an incoherence property [4]. For CS-MRI, it is possible to accurately reconstruct MR images from undersampled k -space data (i.e., partial Fourier data) by solving nonlinear optimization problems.

Suppose that $u' \in \mathbf{R}^N$ is a sparse or compressive representation for a signal $u \in \mathbf{R}^N$ with respect to basis Ψ , i.e., $u' = \Psi u$. Let $K = \|u'\|_0$ be the number of nonzero elements in u' and let H be the $M \times N$ ($K < M \ll N$) measurement

2010 *Mathematics Subject Classification.* Primary: 65N20, 97M10, 97M60; Secondary: 65Q30.

Key words and phrases. Compressive sensing, alternating minimization method, weighted average, magnetic resonance image reconstruction.

The first author is supported by National Natural Science Foundation of China (No. 11271126), Key Project of the Chinese Ministry of Education (No. 109030) and Science Research Project of CUC (XNL1203, XNL1304).

matrix such that $Hu = b$, where b is an observed data vector. Then recovery of u from b can be obtained by solving the L_0 problem

$$\min_u \{\|\Psi u\|_0 : Hu = b\}. \quad (1)$$

However, (1) is provably NP-hard [22] and is very difficult to solve from a numerical computation viewpoint. Thus, it is more realistic to solve the L_1 problem

$$\min_u \{\|\Psi u\|_1 : Hu = b\}, \quad (2)$$

which has also been known to yield sparse solutions under some conditions [10, 13].

In the case of CS-MRI, H is a partial Fourier matrix, i.e., $H = PF$, $P \in \mathbf{R}^{M \times N}$ consists of $M \ll N$ rows of the identity matrix, and F is a discrete Fourier matrix. When b is contaminated with noise such as Gaussian noise of variance σ^2 , the relaxation form for (2) is given by

$$\min_u \{\|\Psi u\|_1 : \|Hu - b\|_2^2 \leq \sigma^2\}. \quad (3)$$

Because (3) is a convex minimization problem, many computational methods can be used to solve it. For example, Bregman iteration [31], the split Bregman method [18], the conjugate gradient method [20], gradient project method [12], coordinate gradient descent method [28], and fast iterative shrinkage-thresholding algorithm [2] are all efficient approaches to solving (3).

Total variation (TV) regularization was first proposed for image denoising by Rudin et al. [24]. A TV regularizer can better preserve sharp edges or boundaries and remove noise in a given image. Therefore, a TV regularizer is a sparsifying transform operator for piecewise smooth MR images. When a TV sparsifying transform and an orthogonal sparsifying transform Ψ are simultaneously considered, the optimization problem in CS MRI can be expressed as

$$\min_u \{\alpha \|u\|_{TV} + \beta \|\Psi u\|_1 : \|Hu - b\|_2^2 \leq \sigma^2\}, \quad (4)$$

where α and β are two positive parameters that control the trade-off between TV sparsity and Ψ sparsity. The unconstrained version of (4) is

$$\min_u \alpha \|u\|_{TV} + \beta \|\Psi u\|_1 + \frac{\mu}{2} \|Hu - b\|_2^2, \quad (5)$$

where μ is a positive parameter that determines the trade-off between the fidelity and sparsity terms and $\|\cdot\|_2$ denotes the Euclidean norm. Model (5) can be equivalently written as

$$\min_u \alpha' \|u\|_{TV} + \beta' \|\Psi u\|_1 + \frac{1}{2} \|Hu - b\|_2^2. \quad (6)$$

Model (5) or (6) can be regarded as a special case of general optimization problems consisting of a loss function and convex functions as priors. Existing methods to solve the generalized problems can be classified into the following types:

- i) Operator-splitting methods: the idea is to find the solution u that makes the sum of the corresponding maximal monotone operators equal to zero. These include forward-backward schemes [6, 14, 27], Douglas-Rachford schemes [25] and projective splitting schemes [11]. The iterative shrinkage thresholding algorithm (ISTA) and fast ISTA (FISTA) [2] are well-known operator-splitting methods. These algorithms are only designed to solve simpler regularization

problems and cannot be efficiently applied to the composite regularization problems (5) and (6) using both L1 and a TV norm.

- ii) Variable splitting methods: these are based on combinations of alternating direction methods (ADMs) under an augmented Lagrangian framework. The augmented Lagrangian method was first used to solve a PDE problem [15, 16]. Tai and Wu [26] and Wang et al. [29] extended the method to solve TV regularization problems. A multiple splitting algorithm (MSA) for convex optimization has also been proposed [17] and Yang et al. developed a splitting algorithm to solve problem (5) or (6) [30]. Zhu and Chern developed a fast alternating minimization method to solve problem (5) [32] and analyzed the convergence of the method [33]. Recently, Zhu and Shi gave a fast method to solve problem (5) or (6) as $\beta = 0$ or $\beta' = 0$ [34]. Chen et al. also used a variable splitting method to solve a CS-MRI variational model [5].
- iii) The composite splitting algorithm: this method combines an operator and a variable splitting technique. Motivated by an effective acceleration scheme [2], an additional acceleration step can be applied to the composite splitting algorithm (CSA). Combining the composite splitting denoising (CSD) method [7, 8] with FISTA [2] yielded the fast composite splitting algorithm (FCSA) [19], which can be used to solve problem (5) or (6) and yields good reconstruction results.

The above-mentioned methods can produce high-quality reconstruction of MR images from partial k -space data. However, the results depend on the given regularization parameters and these methods only consider the case of weak noise. The aim of the present study was to propose a weighted-average alternating formulation with L1 and TV regularization to reconstruct MR images via flexible parameter selection.

We use positive parameters α_1 and α_2 to change (6) to the following model:

$$\min_{u,v,w} \alpha_1 \|u - v\|_2^2 + \alpha_2 \|v - w\|_2^2 + \alpha' \|w\|_{TV} + \beta' \|\Psi w\|_1 + \frac{1}{2} \|Hu - b\|_2^2. \quad (7)$$

It is well known that model (7) reduces to model (6) when the parameters α_1 and α_2 go to infinity. By finding an optimization solution for model (7), we can reconstruct MR images from undersampled k -space (i.e., partial Fourier data). The reconstructed results are compared with those reconstructed by FCSA [19]. The motivation that the model (6) has been changed into model (7) is the better reconstructed images can be obtained by flexible choice of the new parameters α_1 and α_2 in model (7). At the same time, the model (7) can also yield better reconstruction results for the case of strong noise than model (6).

The remainder of the paper is organized as follows. In Section 2, a weighted-average alternating minimization method (WAAMM) to solve (7) is developed. Section 3 presents a convergence analysis of the weighted-average alternating minimization method. In Section 4, the advantages of and the motivation for the proposed method are described. In Section 5, we use real MR images in numerical experiments to demonstrate the effectiveness of WAAMM.

2. Weighted-average alternating minimization method to solve model (7).

In this section, we develop a weighted-average alternating minimization method

to solve model (7). Starting from an initial guess $v^{(0)}$, model (7) computes a sequence of iterates

$$u^{(1)}, w^{(1)}, v^{(1)}, u^{(2)}, w^{(2)}, v^{(2)}, \dots, u^{(k)}, w^{(k)}, v^{(k)}, \dots,$$

in which

$$S_u(v^{(k-1)}) := u^{(k)} = \arg \min_u \alpha_1 \|u - v^{(k-1)}\|_2^2 + \frac{1}{2} \|Hu - b\|_2^2,$$

$$S_w(v^{(k-1)}) := w^{(k)} = \arg \min_w \alpha' \|w\|_{TV} + \beta' \|\Psi w\|_1 + \alpha_2 \|v^{(k-1)} - w\|_2^2$$

and

$$S_v(u^{(k)}, w^{(k)}) := v^{(k)} = \arg \min_v \alpha_1 \|u^{(k)} - v\|_2^2 + \alpha_2 \|v - w^{(k)}\|_2^2$$

for $k = 1, 2, \dots$. Therefore, we can obtain the following relationship between $v^{(k)}$ and $v^{(k-1)}$:

$$v^{(k)} = S_v(u^{(k)}, w^{(k)}) = S_v(S_u(v^{(k-1)}), S_w(v^{(k-1)})), \quad k = 1, 2, \dots$$

For the sake of simplicity, let

$$v^{(k)} = T(v^{(k-1)}), \quad (8)$$

where

$$T(\cdot) = S_v(S_u(\cdot), S_w(\cdot)).$$

In the next section, the convergence of $v^{(k)}$ obtained by the operator T is analyzed.

Now we show how to compute S_u, S_w and S_v in detail. The problem

$$\min_u \alpha_1 \|u - v^{(k-1)}\|_2^2 + \frac{1}{2} \|Hu - b\|_2^2 \quad (9)$$

can be regarded as a deblurring problem. Its optimality condition is

$$2\alpha_1(u - v^{(k-1)}) + H^T(Hu - b) = 0. \quad (10)$$

Substituting $H = PF$ into (10), we have

$$2\alpha_1 u - 2\alpha_1 v^{(k-1)} + F^T P^T P F u - F^T P^T b = 0. \quad (11)$$

Applying operator F to (11) and using the orthogonality of F , we obtain

$$2\alpha_1 F u - 2\alpha_1 F v^{(k-1)} + P^T P F u - P^T b = 0.$$

That is,

$$(2\alpha_1 I + P^T P) F u = P^T b + 2\alpha_1 F v^{(k-1)}.$$

Because $2\alpha_1 I + P^T P$ is a diagonal matrix, it is easy to solve $F u$. Then, F^T operation (i.e. inverse Fourier transform) will yield u . Therefore, computation of $u^{(k)}$ is fast.

The problem

$$\min_w \alpha' \|w\|_{TV} + \beta' \|\Psi w\|_1 + \alpha_2 \|v^{(k-1)} - w\|_2^2 \quad (12)$$

can be changed to

$$\min_w \frac{1}{2\frac{1}{\alpha_2}} \|w - v^{(k-1)}\|_2^2 + \frac{\alpha'}{2} \|w\|_{TV} + \frac{\beta'}{2} \|\Psi w\|_1. \quad (13)$$

Problem (13) can be considered as a denoising problem and can be solved using a proximal map. For a continuous convex function $g(w)$ and any scalar $\tau > 0$, the proximal map associated with function $g(w)$ is defined as follows [1, 2]:

$$\text{prox}_\tau(g)(v) := \arg \min_w \left\{ g(w) + \frac{1}{2\tau} \|w - v\|^2 \right\}. \tag{14}$$

Therefore, the minimizer for denoising problem (13) can be expressed as

$$\text{prox}_{\frac{1}{\alpha_2}}(g)(v^{(k-1)}) := \arg \min_w \left\{ g(w) + \frac{1}{2\frac{1}{\alpha_2}} \|w - v^{(k-1)}\|^2 \right\}, \tag{15}$$

where $g(w) = \frac{\alpha'}{2} \|w\|_{TV} + \frac{\beta'}{2} \|\Psi w\|_1$.

In section 6, we will use the composite of the fast gradient-based algorithm for constrained total variation image denoising in [1] and fast iterative shrinkage thresholding algorithm in [2] to solve (15). So to compute $v^{(k)}$ is also fast.

The optimality condition for the problem

$$\min_v \alpha_1 \|u^{(k)} - v\|_2^2 + \alpha_2 \|v - w^{(k)}\|_2^2, \tag{16}$$

is

$$2\alpha_1 (v - u^{(k)}) + 2\alpha_2 (v - w^{(k)}) = 0. \tag{17}$$

$$v^{(k)} = \frac{\alpha_1 u^{(k)} + \alpha_2 w^{(k)}}{\alpha_1 + \alpha_2}. \tag{18}$$

Obviously, we can obtain the exact $v^{(k)}$ by $u^{(k)}$ and $w^{(k)}$. Since $v^{(k)}$ is the weighted average of $u^{(k)}$ and $w^{(k)}$, the above method is called a weighted-average alternating minimization method.

3. Convergence analysis. In this section, we present a convergence analysis of the proposed method.

Theorem 3.1. *The operator $S_u(\cdot)$ is contractive, that is, for $x, y \in \mathbb{R}^{n^2}$, it holds that*

$$\|S_u(x) - S_u(y)\|_2 \leq \rho \|x - y\|_2,$$

where $0 < \rho < 1$.

Proof.

$$\begin{aligned} & \|S_u(x) - S_u(y)\|_2 \\ &= \left\| (2\alpha_1 I + H^T H)^{-1} (2\alpha_1 x + H^T b) - (2\alpha_1 I + H^T H)^{-1} (2\alpha_1 y + H^T b) \right\|_2 \\ &\leq \left\| 2\alpha_1 (2\alpha_1 I + H^T H)^{-1} \right\|_2 \|x - y\|_2. \end{aligned}$$

Let $\rho = \left\| 2\alpha_1 (2\alpha_1 I + H^T H)^{-1} \right\|_2$. Since $2\alpha_1 I + H^T H$ is symmetric positive definite and its eigenvalues are greater than $2\alpha_1$, we have

$$\|S_u(x) - S_u(y)\|_2 \leq \rho \|x - y\|_2.$$

This completes the proof. □

Theorem 3.2. *The operator $S_w(\cdot)$ is firmly nonexpansive, i. e. , $\forall(x, y) \in \mathbb{R}^{n^2} \times \mathbb{R}^{n^2}$,*

$$\|S_w(x) - S_w(y)\|_2 \leq \|x - y\|_2.$$

The proof of the theorem is easily obtained using Lemma 2.4 in [6]. And the proof of this theorem is originally provided in [21].

Next we show that the operator T is contractive.

Theorem 3.3. *The operator T defined in (8) is contractive.*

Proof.

$$\begin{aligned} & \|T(x) - T(y)\|_2 \\ &= \|S_v(S_u(x), S_w(x)) - S_v(S_u(y), S_w(y))\|_2 \\ &= \left\| \frac{\alpha_1 S_u(x) + \alpha_2 S_w(x)}{\alpha_1 + \alpha_2} - \frac{\alpha_1 S_u(y) + \alpha_2 S_w(y)}{\alpha_1 + \alpha_2} \right\|_2 \\ &\leq \frac{\alpha_1}{\alpha_1 + \alpha_2} \|S_u(x) - S_u(y)\|_2 + \frac{\alpha_2}{\alpha_1 + \alpha_2} \|S_w(x) - S_w(y)\|_2. \end{aligned}$$

By Theorems 3.1 and 3.2, we have

$$\|T(x) - T(y)\|_2 \leq \frac{\rho\alpha_1 + \alpha_2}{\alpha_1 + \alpha_2} \|x - y\|_2.$$

Let $\rho' = \frac{\rho\alpha_1 + \alpha_2}{\alpha_1 + \alpha_2}$. Then $0 < \rho' < 1$ and $\|T(x) - T(y)\|_2 \leq \rho' \|x - y\|_2$.

This confirms the contractiveness of the operator $T(\cdot)$.

For any initial guess $v^{(0)} \in \mathbb{R}^{n^2}$, suppose that $\{v^{(k)}\}$ is generated by (8). Then T is asymptotically regular, that is,

$$\lim_{k \rightarrow \infty} \|v^{(k+1)} - v^{(k)}\|_2 = \lim_{k \rightarrow \infty} \|T^{(k+1)}(v^{(0)}) - T^{(k)}(v^{(0)})\|_2 = 0.$$

Let $G(u, v, w) = \alpha_1 \|u - v\|_2^2 + \alpha_2 \|v - w\|_2^2 + \alpha' \|w\|_{TV} + \beta' \|\Psi w\|_1 + \frac{1}{2} \|Hu - b\|_2^2$. Then $G(u, v, w)$ is the objective function in (7). It is convex, bounded below, and coercive, and thus (7) has at least one minimizer (u^*, v^*, w^*) and must satisfy

$$u^* = S_u(v^*),$$

$$w^* = S_w(v^*),$$

and

$$v^* = S_v(u^*, w^*).$$

Therefore, v^* is a fixed point of T .

According to the Opial theorem [23], the sequence $\{v^{(k)}\}$ converges to a fixed point of \mathcal{T} , that is, a minimizer of G . □

4. Further explanation of the weighted-average alternating minimization method. In this section, we explain the motivation for and the advantages of the proposed method.

We know that model (7) can reduce to model (6) if the regularization parameters α_1 and α_2 approach to infinity. Thus, if α_1 and α_2 are chosen sufficiently large in problem (7), we can force $u = v$ and $v = w$. This is consistent with problem (6). However, the solution of (6) is fixed once the parameters α' and β' are given, and it is not necessarily an optimal reconstructed result for an MR image from partial k -space data. After model (7) replaces model (6) with the fixed parameters α' and β' , we can obtain better reconstructed images than model (6) by appropriate choice of the new parameters α_1 and α_2 in model (7). According to (18), the solution of (7) is obtained as a weighted average of the solution of deblurring problem (9) and the solution of denoising problem (13). The coefficient $\frac{\alpha_1}{\alpha_1 + \alpha_2}$ is the weight for the solution of the deblurring problem, and $\frac{\alpha_2}{\alpha_1 + \alpha_2}$ is the weight for the solution of the denoising problem. Therefore, we can choose values of α_1 and α_2 according to the level of noise to reconstruct MR images from partial k -space data.

The numerical experimental results in the next section demonstrate that this qualitative analysis is correct. In particular, in the case of strong noise, adjustment of α_1 and α_2 in model (7) leads to an advantage over model (6). Some real MR reconstruction experiments confirm that model (7) can yield better reconstruction of MR images from partial Fourier data than model (6).

5. Numerical experiments. In this section, we assess the WAAMM performance for CS-MRI. We compare our method with FCSA [19], the standard method for CS-MRI.

The signal to noise ratio (SNR) and relative error (ReErr) are used to measure the quality of the reconstructed images. These are defined as

$$\text{SNR} = 10 \log 10 \left(\frac{\|u_0\|_2}{\|u_0 - u\|_2} \right) \tag{19}$$

and

$$\text{ReErr} = \frac{\|u - u_0\|_2^2}{\|u_0\|_2^2}, \tag{20}$$

where u and u_0 denote the reconstructed and original images, respectively. The CPU time is used to evaluate the speed of MRI reconstruction. All experiments were performed in MATLAB on a laptop with an Intel Core Duo P8400 processor and 2 GB of memory.

First, we consider the case of weak noise and assume that the mean and standard deviation for additive Gaussian noise are 0 and 0.01, respectively. The sparse basis Ψ is chosen as the Haar wavelet. In reconstruction tests with the two methods, we choose $\alpha' = 0.001$, $\beta' = 0.035$, and set the initial image u_0 to zero. In tests for WAAMM, we choose $\alpha_1 = 2^{10}$ and $\alpha_2 = 2^8$. In addition, since reconstructed results are obtained from partial Fourier data, the solution of problem (7) mainly comprises the solution to the deblurring problem. Thus, α_1 must be greater than α_2 in numerical experiments using model (7). For the stopping criterion, the relative difference between successive iterates for the reconstructed image should satisfy the following inequality:

$$\frac{\|u^{(k)} - u^{(k-1)}\|_2}{\|u^{(k)}\|_2} < 10^{-3}. \tag{21}$$

The reason of choosing less than 10^{-3} is the two methods are up to the convergence. Using these parameters and stopping criterion, we applied our method for reconstruction of a brain MR image. Fig. 1. (a) is a real brain MR image of 600×600 in size. Fig. 1. (b) shows 88 radial lines in the frequency space for this image. If the brain image is sampled using 88 views in the frequency space, then the sampling rate is 15.993%.

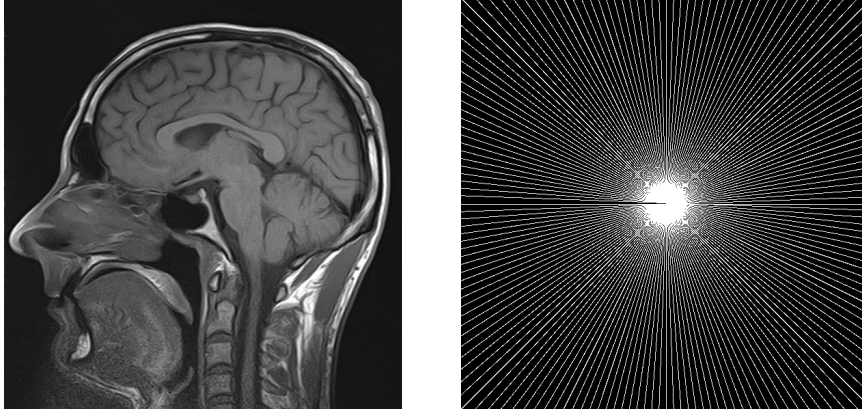


Fig. 1. (a) Original image.

(b) The 88 views in the frequency space.

The reconstructed image after the stopping criterion is satisfied is shown in Fig. 2. (a). The SNR, ReErr and CPU time are 23.2095 dB, 0.0376 and 11.5156 s, respectively. The reconstruction error magnitude, i. e., $|x - x_o|$, are presented in Fig. 2. (c) and Fig. 2. (d). x is reconstructed image and x_o is the original image. The reconstruction error magnitude for WAAMM shows lower pixel errors than for FCSA.

We used FCSA for brain MRI reconstruction using the same sampling ratio. The result is presented in Fig. 2. (b). The SNR, ReErr and CPU time are 22.7699 dB, 0.0396 and 21.4531 s, respectively.



(a) Reconstruction by WAAMM.



(b) Reconstruction by FCSA.

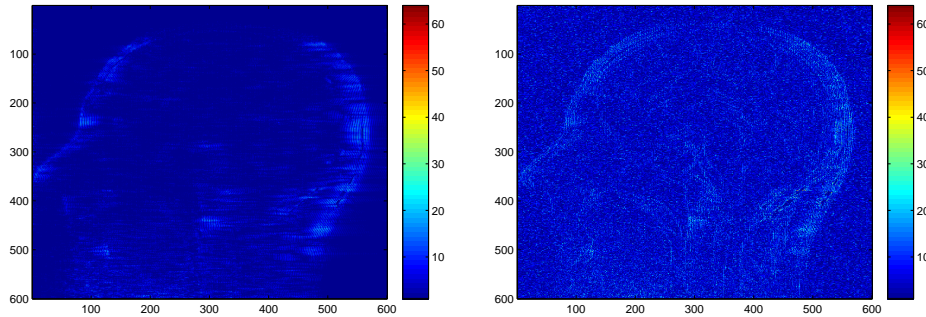
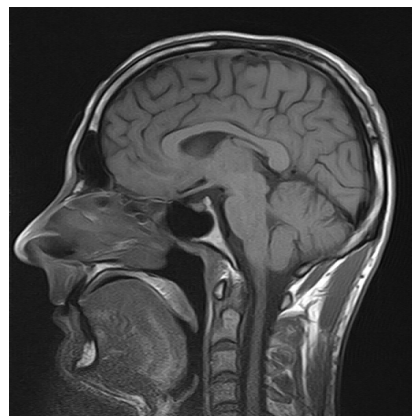


Fig. 2. (c) Reconstruction error magnitude for WAAMM. (d) Reconstruction error magnitude for FCSA.

From the two reconstructed images it is clear that the WAAMM method is slightly better than FCSA in the case of weak noise. We increased the standard deviation for noise to 1000 and performed reconstruction tests with the two methods using the same α_1 and α_2 parameters and sampling views. The WAAMM and FCSA reconstruction results and corresponding magnitude of reconstruction errors are shown in Fig. 3. The SNR, ReErr, and CPU time are 22.4322 and 21.2365 dB, 0.0412 and 0.0472, and 11.8750 and 28.8281 s for WAAMM and FCSA, respectively. The results reveal that WAAMM is better than FCSA since the SNR is greater for WAAMM than for FCSA while the CPU time for WAAMM is less than for FCSA.



(a) Reconstruction by WAAMM.



(b) Reconstruction by FCSA.

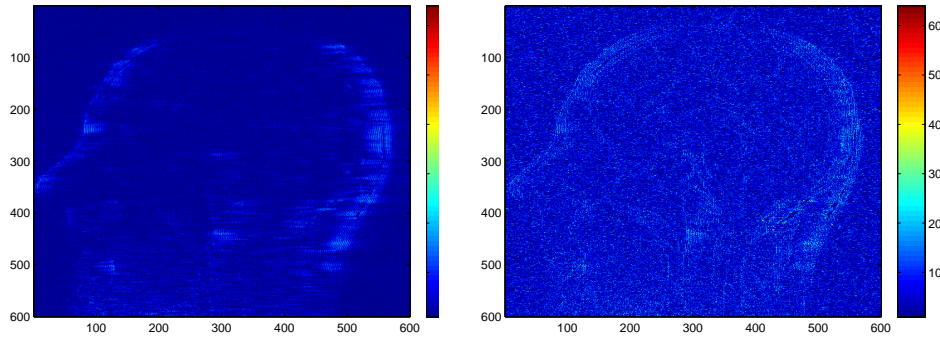


Fig. 3. (c) Reconstruction error magnitude for WAAMM. (d) Reconstruction error magnitude for FCSA.

Table 1 lists values for the SNR, ReErr and CPU time for results reconstructed by WAAMM ($\alpha_1 = 2^{10}$, $\alpha_2 = 2^8$) and FCSA when the stopping criterion is satisfied for a sampling rate of 15.993% and standard deviation of 1000–5000.

Table 1. SNR, ReErr and CPU time for WAAMM and FCSA reconstruction results

Standard deviation	Method	SNR (dB)	ReErr	CPU (s)
1000	WAAMM	22.4322	0.0412	11.8750
	FCSA	21.2365	0.0472	28.8281
1500	WAAMM	21.6232	0.0452	13.6250
	FCSA	20.3865	0.0521	30.6094
2000	WAAMM	20.6960	0.0503	15.0625
	FCSA	19.4644	0.0579	31.8594
2500	WAAMM	19.7364	0.0561	16.6875
	FCSA	18.5341	0.0645	33.3125
3000	WAAMM	18.7942	0.0626	18.1094
	FCSA	17.6290	0.0716	34.5938
3500	WAAMM	17.8936	0.0694	19.6250
	FCSA	16.7670	0.0790	36.3750
4000	WAAMM	17.0437	0.0765	21.5156
	FCSA	15.9535	0.0868	37.4844
4500	WAAMM	16.2467	0.0839	23.1563
	FCSA	15.1884	0.0948	39.2031
5000	WAAMM	15.5005	0.0914	24.3906
	FCSA	14.4702	0.1029	40.5625

The results reveal that WAAMM yields better reconstruction results than FCSA does. If we increase α_2 to 2^9 , we can obtain a better result. For example, for standard deviation of 3500, 88 sampling views, $\alpha_1 = 2^{10}$ and $\alpha_2 = 2^8$, the SNR, ReErr and CPU time for WAAMM are 17.8936 dB, 0.0694 and 19.6250 s, respectively. For α_1 fixed and an increase in α_2 to 2^9 , the SNR, ReErr and CPU time for the WAAMM reconstruction result are 17.9031 dB, 0.0693 and 18.1093 s, respectively. Table 2 lists the WAAMM performance results for different values of α_2 .

Table 2. SNR, ReErr and CPU time for the WAAMM reconstruction results for different values of α_2

α_2	SNR(dB)	ReErr	CPU (s)
2^6	17.8886	0.0695	23.0156
2^7	17.8913	0.0694	21.2656
2^8	17.8936	0.0694	19.6250
2^9	17.9031	0.0693	18.1093
2^{10}	15.6733	0.0896	19.6563
2^{11}	13.0344	0.2041	23.6406

The data reveal that the reconstructed results can be improved by adjusting α_2 . When the value of α_2 is greater than or equal to α_1 , the SNR for the reconstructed results starts to decrease. The reason is that the reconstructed image is mainly obtained from partial Fourier data, as discussed above. In addition, if α_1 and α_2 are changed to different values, the quality of the reconstructed images can be improved. For example, a reconstructed image for $\alpha_1 = 2^6$ and $\alpha_2 = 2^5$ is shown in Fig. 4. (a). The SNR, ReErr and CPU time are 17.9073 dB, 0.0692 and 15.5781 s, respectively. Fig. 4. (b) shows the corresponding FCSA result. Fig. 4. (c) and Fig. 4. (d) show the reconstruction error magnitudes for WAAMM and FCSA. The SNR, ReErr and CPU time are 15.4461 dB, 0.0920 and 56.9218 s, respectively. Obviously, the WAAMM result is better than the FCSA reconstruction and the proposed method is very well suited to the case of strong noise and can improve image reconstruction via flexible parameter selection. Identification of the optimal parameter in reconstruction experiments is beyond the scope of the current study and will be addressed in future research.



(a) Reconstruction by WAAMM.



(b) Reconstruction by FCSA.

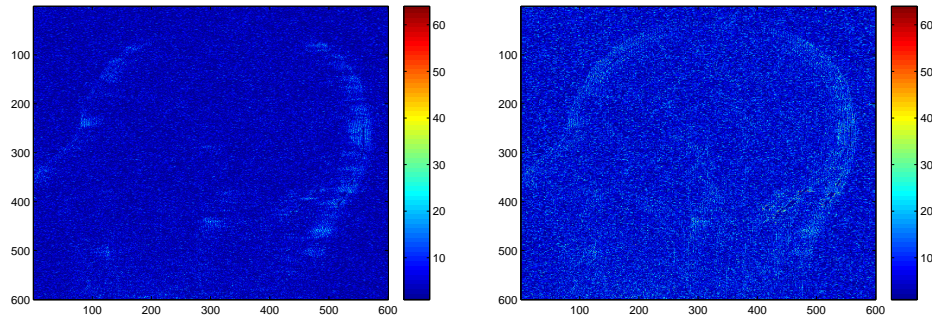


Fig. 4. (c) Reconstruction error magnitude for WAAMM. (d) Reconstruction error magnitude for FCSA.

Acknowledgments. We would like to thank the referees for making helpful suggestions.

REFERENCES

- [1] A. Beck and M. Teboulle, [Fast gradient-based algorithms for constrained total variation image denoising and deblurring problems](#), *IEEE Transaction on Image Processing*, **5** (2009), 2419–2434.
- [2] A. Beck and M. Teboulle, [A fast iterative shrinkage-thresholding algorithm for linear inverse problems](#), *SIAM Journal on Imaging Sciences*, **2** (2009), 183–202.
- [3] E. J. Candès, J. Romberg and T. Tao, [Robust uncertainty principles: Exact signal reconstruction from highly incomplete frequency information](#), *IEEE Transactions on Information Theory*, **52** (2006), 489–509.
- [4] E. J. Candès and J. Romberg, [Sparsity and incoherence in compressive sampling](#), *Inverse Problems*, **23** (2007), 969–985.
- [5] Y. Chen, X. Ye and F. Huang, [A novel method and fast algorithm for MR image reconstruction with significantly under-sampled data](#), *Inverse Problems and Imaging*, **4** (2010), 223–240.
- [6] P. L. Combettes and V. R. Wajs, [Signal recovery by proximal forward-backward splitting](#), *Multiscale Modeling and Simulation*, **4** (2005), 1168–1200.
- [7] P. L. Combettes, [Iterative construction of the resolvent of a sum of maximal monotone operators](#), *Journal of Convex Analysis*, **16** (2009), 727–748.
- [8] P. L. Combettes and J.-C. Pesquet, [A proximal decomposition method for solving convex variational inverse problems](#), *Inverse Problems*, **24** (2008), 065014, 27 pp.
- [9] D. L. Donoho, [Compressed sensing](#), *IEEE Transactions on Information Theory*, **52** (2006), 1289–1306.
- [10] D. L. Donoho and X. Huo, [Uncertainty principles and ideal atomic decompositions](#), *IEEE Transactions on Information Theory*, **47** (2001), 2845–2862.
- [11] J. Eckstein and B. F. Svaiter, [General projective splitting methods for sums of maximal monotone operators](#), *SIAM Journal on Control Optimization*, **48** (2009), 787–811.
- [12] M. Figueiredo, R. Nowak and S. Wright, [Gradient projection for sparse reconstruction: application to compressed sensing and other inverse problems](#), *IEEE Journal of Selected Topics in Signal Processing*, **1** (2007), 586–597.
- [13] J.-J. Fuchs, [On sparse representations in arbitrary redundant bases](#), *IEEE Transactions on Information Theory*, **50** (2004), 1341–1344.
- [14] D. Gabay, [Chapter IX applications of the method of multipliers to variational inequalities](#), *Studies in Mathematics and its Applications*, **15** (1983), 299–331.
- [15] D. Gabay and B. Mercier, [A dual algorithm for the solution of nonlinear variational problems via finite element approximations](#), *Computers and Mathematics with Applications*, **2** (1976), 17–40.
- [16] R. Glowinski and P. Le Tallec, [Augmented Lagrangian and Operator-Splitting Methods in Nonlinear Mechanics](#), SIAM Studies in Applied Mathematics, 9, Society for Industrial Mathematics (SIAM), Philadelphia, PA, 1989.

- [17] D. Goldfarb and S. Ma, [Fast multiple-splitting algorithms for convex optimization](#), *SIAM Journal on Optimization*, **22** (2012), 533–556
- [18] T. Goldstein and O. Osher, [The split Bregman method for L1-regularized problems](#), *SIAM Journal on Imaging Sciences*, **2** (2009), 323–343.
- [19] J. Huang, S. Zhang and D. Metaxas, [Efficient MR image reconstruction for compressed MR imaging](#), in *Medical Image Computing and Computer-Assisted Intervention–MICCAI 2010*, Lecture Notes in Computer Science, 6361, Springer-Verlag, Berlin Heidelberg, 135–142.
- [20] M. Lustig, D. L. Donoho and J. Pauly, [Sparse MRI: The application of compressed sensing for rapid MR imaging](#), *Magnetic Resonance in Medicine*, **58** (2007), 1182–1195.
- [21] J.-J. Moreau, Proximité et dualité dans un espace hilbertien, *Bull. Soc. Math. France*, **93** (1965), 273–299.
- [22] B. K. Natarajan, [Sparse approximate solutions to linear systems](#), *SIAM Journal on Computing*, **24** (1995), 227–234.
- [23] Z. Opal, [Weak convergence of the sequence of successive approximations for nonexpansive mappings](#), *Bull. Amer. Math. Soc.*, **73** (1967), 591–597.
- [24] L. Rudin, S. Osher and E. Fatemi, [Nonlinear total variation based noise removal algorithms](#), *Physica D*, **60** (1992), 259–268.
- [25] J. E. Spingarn, [Partial inverse of monotone operator](#), *Applied Mathematics and Optimization*, textbf10 (1983), 247–265.
- [26] X. C. Tai and C. Wu, [Augmented Lagrangian method, dual methods and split Bregman iteration for ROF model](#), in *Scale Space and Variational Methods in Computer Vision*, Lecture Notes in Computer Science, 5567, Springer, Berlin Heidelberg, 2009, 502–513.
- [27] P. Tseng, [A modified forward-backward splitting method for maximal monotone mappings](#), *SIAM Journal on Control and Optimization*, **38** (2000), 431–446.
- [28] P. Tseng and S. Yun, [A coordinate gradient descent method for nonsmooth separable minimization](#), *Math. Prog. B.*, **117** (2009), 387–423.
- [29] Y. Wang, J. Yang, W. Yin and Y. Zhang, [A new alternating minimization algorithm for total variation image reconstruction](#), *SIAM Journal on Imaging Sciences*, **1** (2008), 248–272.
- [30] J. Yang, Y. Zhang and W. Yin, [A fast alternating direction method for TV-L1-L2 Signal reconstruction from partial Fourier data](#), *IEEE Journal of Selected Topics in Signal Processing*, **4** (2010), 288–297.
- [31] W. Yin, S. Osher, D. Goldfarb and J. Darbon, [Bregman Iterative algorithms for \$l_1\$ -minimization with applications to compressed sensing](#), *SIAM Journal on Imaging Sciences*, **1** (2008), 143–168.
- [32] Y. Zhu and I. Chern, [Fast alternating minimization method for compressive sensing MRI under wavelet sparsity and TV sparsity](#), in *2011 Sixth International Conference on Image and Graphics*, IEEE, 2011, 356–361.
- [33] Y. Zhu and I. Chern, [Convergence of the alternating minimization method for sparse MR image reconstruction](#), *Journal of Information and Computational Science*, **8** (2011), 2067–2075.
- [34] Y. Zhu and Y. Shi, [A fast method for reconstruction of total-variation MR images with a periodic boundary condition](#), *IEEE Signal Processing Letters*, **20** (2013), 291–294.

Received August 2012; revised August 2013.

E-mail address: ygzhu@cuc.edu.cn

E-mail address: yyshi@ncepu.edu.cn

E-mail address: zhangbin628@cuc.edu.cn

E-mail address: yuxinyan@cuc.edu.cn